The variable analysis of an MHD generator with electrical output of 10 kW for application to bi-plant method electricity generation

Authors: Lee, G., & Kim, H.R*.

Journal Information:

- **Journal:** International Journal of Energy Research
- **Year:** 2020
- **Volume:** 44(10)
- **Pages:** 8125-8132
- **DOI:** https://doi.org/10.1002/er.5100

The variable analysis of an MHD generator with electrical output of 10 kW for application to bi-plant method electricity generation

Geun Hyeong Lee, Hee Reyoung Kim*

Ulsan National Institute of Science and Technology, Department of Nuclear Engineering, Ulsan 689-798, Republic of Korea

Abstract

Magnetohydrodynamic (MHD) generators can be used to increase the total efficiencies of fossil power plants by adopting a bi-plant design, in which electricity is generated using both a turbine and the MHD generator. An MHD generator with an electric output of 10 kW is numerically analyzed herein for application to bi-plant method electricity generation. An electrically conductive plasma flue gas, with a high temperature of approximately 3000 K from the power plant, was considered for the generation of electricity from its flow in the magnetic field, where electricity was produced directly without the turbine facility from the MHD generator. Velocity profiles were calculated using an ANSYS code simulation. Then, using the magnetic flux density, the electrical output was calculated to design the MHD generator. The magnetic flux density, velocity, and geometrical variables affected the power output of the MHD generator. The power was proportional to the square of magnetic flux density, whereas velocity and power density were constant.

Keywords: Magnetohydrodynamic generator; Magnetic flux density; Velocity; Electrical output

Nomenclatures

$\vec{B}$ Magnetic flux density [T]

d	Duct distance horizontal x-direction [m]
$\vec{E}$	Electric field [kg·m/(s^3·A)]
$\vec{F}$	Lorentz force [kg·m/s^2]
I	Total current [A]
I_k	Short circuit current [A]
i	Relative current
$\vec{J}$	Current density [A/m^2]
p	Developed system pressure [Pa]
q	Charge [C]
R_i	Internal resistance [Ω]
R_L	Load resistance [Ω]
t	Time [s]
$\vec{U}$	Fluid velocity [m/s]
V	Total voltage [kg·m^2/(s^3·A)]
v	Volume of fluid [m^3]
V_0	Voltage across the fluid [kg·m^2/(s^3·A)]
W	Total power [W]
W_{in}	Input power [W]
W_{max}	Maximum power [W]
W_{out}	Output power [W]
W_e	Drift velocity [m/s]
ε_0	Electrical permittivity in vacuum [F/m] (8.85×10^{-12})
μ_0	Magnetic permeability in vacuum [H/m] (1.257×10^{-6})
ν	Kinematic viscosity [m^2/s]

ρ Density [kg/m^3]

σ Electrical conductivity [$1/(\Omega \cdot m)$]

ω Cyclotron frequency [1/s]

τ Free flight time of the electrons [s]

β Hall parameter

η Efficiency

1. INTRODUCTION

Coal will be the only fossil fuel resource available by the mid- to late this century due to depletion of oil, natural gas, and uranium. Hence, the development of efficient coal-fired power generation technologies is necessary to meet the energy demands of the future. However, the environmental problems caused by slag occurring during the combustion process of coal, and sulfur oxides and nitrogen oxides should not be overlooked. Magnetohydrodynamic (MHD) systems are being considered as an alternative method to meet the energy demands of the future.

The basic operating principle of the MHD generator is the interaction between a magnetic field and an electrically conducting fluid. The MHD generator converts kinetic and heat energy directly into electricity using plasma as a fluid and can operate at high temperatures compared to other generator technologies. The combination of MHD power generators with steam power generators, called the 'Bi-plant method', results in a highly efficient power generation technology for the conversion of fossil fuel energy into electricity. The efficiency can reach 40% to 60% or more.[1] In addition, the MHD generator can eliminate harmful gases such as carbon dioxide (CO_2), nitrogen oxides (NO_x), and sulfur oxides (SO_x) due to plasma interactions.[2] However, the disadvantage of MHD generator systems is their high operating temperatures. Heat exchangers are needed to generate plasma at such high temperatures.

MHD generators can be divided into open- and closed-cycle systems according to their thermodynamic cycles. The open-cycle system employs the Brayton cycle, in which the thermodynamic operating fluid completes the cycle in the gaseous state. The closed-cycle system employs the Rankine cycle, in which the thermodynamic operating fluid circulates through condensation. An open-cycle system allows high-temperature combustion gases to pass directly through the MHD generator, and a closed-cycle MHD generator uses combustion heat from fossil fuels to develop noble gases[3]. In this study, an open-cycle MHD generator system is considered.

In an MHD generator, high heat energy remains after generation because it operates at high temperatures. Therefore, a combined plant method is used to utilize the remaining heat, thus generating more energy and thereby increasing efficiency. The principle of operation for a combined open-cycle MHD generator system is the addition of a fuel and seed to the combustor. The 1st electrical output (DC) is produced through the MHD generator using the heat generated from the combustor, as shown in Fig. 1. The preheated air from the emitted gas of the MHD generator is then used in a steam generator to generate the 2nd electrical output (AC), and the seed is recovered to recirculate the system.

The MHD generator device can be separated into a Faraday current generator and a Hall current generator[4]. In this research, we examined the basic characteristics of the Faraday-type generator because its geometry is relatively simple, and therefore, its reliability is relatively high compared to Hall-type generators.[3] The electric power of 10 kW MHD was adopted to adjust to the laboratory scale size. We analyzed electromagnetic, hydraulic, and geometrical parameters to determine the MHD characteristics for developing an open-cycle system.

2. ANALYSIS OF MHD GENERATOR

The Faraday-type MHD generator, shown in Fig. 2, is analyzed herein.[4,5] In this study, a plasma offgas at 3000 K is used to give electrical conductivity to the plasma fluid required to generate electricity.[6,7] The plasma fluid flows in the x-direction, and the magnetic flux is directed along the z-axis. Subsequently, the current is generated in the y-direction. The basic equations to solve for the parameters of the MHD generator are the Maxwell equations and Navier–Stokes equation.[8] The four vector relations of the Maxwell equations and Navier–Stokes equation for the MHD are expressed as[9]:

$$\text{Ampere's law: } \nabla \times \vec{B} = \mu_0 \left(\vec{J} + \varepsilon_0 \frac{\partial \vec{E}}{\partial t}\right); \tag{1}$$

$$\text{Faraday's law: } \nabla \times \vec{E} = -\frac{\partial \vec{B}}{\partial t}; \tag{2}$$

$$\text{Gauss's law for magnetism: } \nabla \cdot \vec{B} = 0; \tag{3}$$

$$\text{Ohm's law: } \vec{J} = \sigma \vec{E}; \tag{4}$$

$$\text{Navier–Stokes equation: } \frac{\partial \vec{U}}{\partial t} + \left(\vec{U} \cdot \nabla\right)\vec{U} = -\frac{1}{\rho}\nabla \vec{p} + \nu \nabla^2 \vec{U} + \frac{1}{\rho}\vec{J} \times \vec{B}. \tag{5}$$

Ohm's law in Eq. (4) can be generalized by considering Lorentz's force and the Hall effect. In a special case, the generalized form is added. First, Lorentz's force law is given by:

$$\vec{F} = q(\vec{U} \times \vec{B}). \tag{6}$$

The motion of the electromotive force is added via the electric field ($\vec{E}$), and the current density is represented by:

$$\vec{J} = \sigma(\vec{E} + \vec{U} \times \vec{B}). \tag{7}$$

The MHD generator system uses a plasma material interacting with a magnetic field such that a drift velocity perpendicular to the magnetic field is formed in the plasma. The Hall field thus generated, is added to the current density in Eq. (7) to yield:

$$\vec{J} = \sigma\left(\vec{E} + \vec{U} \times \vec{B}\right) - \sigma(\overrightarrow{W_e} \times \vec{B}). \tag{8}$$

The first hall field term ($\sigma \overrightarrow{W_e}$) is given by[10]:

$$\sigma \overrightarrow{W_e} = \mu_0 \vec{J} = \frac{\omega \tau}{|B|}\vec{J} = \frac{\beta}{|B|}\vec{J}. \tag{9}$$

Finally, the generalized Ohm's law for an MHD generator is given by[11]:

$$\vec{J} = \sigma\left(\vec{E} + \vec{U} \times \vec{B}\right) - \frac{\beta}{|B|}(\vec{J} \times \vec{B}). \tag{10}$$

In the Cartesian coordinate system, the components of Eq. (10) are represented as:

$$J_{\mathrm{x}} = \sigma\left(E_{\mathrm{x}} + U_{\mathrm{y}}B_{\mathrm{z}} - U_{\mathrm{z}}B_{\mathrm{y}}\right) - \frac{\beta}{|B|}(J_{\mathrm{y}}B_{\mathrm{z}} - J_{\mathrm{z}}B_{y}), \tag{11}$$

$$J_{\mathrm{y}} = \sigma\left(E_{\mathrm{y}} + U_{\mathrm{x}}B_{\mathrm{z}} - U_{\mathrm{z}}B_{\mathrm{x}}\right) - \frac{\beta}{|B|}(J_{\mathrm{x}}B_{\mathrm{z}} - J_{\mathrm{z}}B_{\mathrm{x}}), \tag{12}$$

$$J_{\mathrm{z}} = \sigma\left(E_{\mathrm{z}} + U_{\mathrm{x}}B_{\mathrm{y}} - U_{\mathrm{y}}B_{\mathrm{x}}\right) - \frac{\beta}{|B|}(J_{\mathrm{x}}B_{\mathrm{y}} - J_{\mathrm{y}}B_{\mathrm{x}}). \tag{13}$$

Eqs. (14) and (15) define the generalized conditions assumed for the MHD generator. Only the *z*-component of the magnetic flux density is considered since the external magnetic field is generally much higher than the *x*- and *y*-components. The drift velocity in z direction is negligible because x- and y-direction of magnetic flux density is negligible.

$$\vec{B} = B_{\mathrm{z}} \tag{14}$$

$$\vec{U} = U_{\mathrm{x}} + U_{y} + U_{z} \tag{15}$$

Subsequently, Eqs. (11)-(13) are arranged with respect to current density in x- and y- direction using the generalized conditions to:

$$J_{\mathrm{x}} = \frac{\sigma}{1-\beta^2}\left\{E_x + U_yB_z - \beta\left(E_y + U_xB_z\right)\right\}, \tag{16}$$

$$J_{\mathrm{y}} = \frac{\sigma}{1-\beta^2}\{E_y + U_xB_z - \beta(E_x + U_yB_z)\}, \tag{17}$$

$$J_{\mathrm{z}} = \sigma E_{\mathrm{z}}. \tag{18}$$

The electric circuit method in Fig. 3 was applied to analyze the MHD generator specifications with different geometrical variables. The graphs of power according to the variables were obtained by the electrical circuit method. The voltage across the fluid from the electromotive force and the current are represented as:

$$V_0 = \mathrm{BU}d, \tag{19}$$

$$I = \frac{\mathrm{BU}}{R_i + R_L}. \tag{20}$$

The short circuit current ($R_{\mathrm{L}} = 0$) is given by:

$$I_k = \frac{\mathrm{BU}d}{R_L}. \tag{21}$$

The relative current is represented as the current ratio between the total current and short circuit current:

$$i = \frac{I}{I_k} = \frac{R_L}{R_i + R_L}. \tag{22}$$

Power output and efficiency can be represented by the function of the current ratio,[12] where maximum power density is achieved when R_i is equal to R_L:

$$W = VI = \mathrm{V_0 I_k}(1 - i)i = \frac{(\mathrm{BU}d)^2 R_i}{(R_i + R_L)^2}, \tag{23}$$

$$W_{max} = VI = \frac{V_0 I_\mathrm{k}}{4} = \frac{(BUd)^2}{4R_L} = \sigma \mathrm{B}^2 U^2 v, \tag{24}$$

$$\eta = \frac{W_{out}}{W_{in}} = \frac{VI}{V_0 I} = 1 - i. \tag{25}$$

The electrical conductivity, magnetic flux density, and geometrical variables were analyzed for lab scale MHD generator.

The finite element method was used to calculate the electromagnetic conditions of MHD generator. The Maxwell equations and the Navier–Stokes equation are represented by Eqs. (26)-(38) for the 3-dimensional nodes.

$$J_x^{i,j,k} = \frac{1}{\mu_0} \frac{\partial B_{\mathrm{n,z}}^{i,j,k}}{\partial y} \tag{26}$$

$$J_y^{i,j,k} = \frac{1}{\mu_0} \frac{\partial B_{\mathrm{n,z}}^{i,j,k}}{\partial x} \tag{27}$$

$$J_z^{i,j,k} = 0 \tag{28}$$

$$\frac{\partial E_{\mathrm{z}}^{i,j,k}}{\partial y} - \frac{\partial E_{\mathrm{y}}^{i,j,k}}{\partial z} = 0 \tag{29}$$

$$\frac{\partial E_{\mathrm{x}}^{i,j,k}}{\partial z} - \frac{\partial E_{\mathrm{z}}^{i,j,k}}{\partial x} = 0 \tag{30}$$

$$\frac{\partial E_{\mathrm{y}}^{i,j,k}}{\partial x} - \frac{\partial E_{\mathrm{x}}^{i,j,k}}{\partial y} = 0 \tag{31}$$

$$\frac{\partial B_z^{i,j,k}}{\partial z} = 0 \tag{32}$$

$$J_x^{i,j,k} = \sigma(E_x^{i,j,k} + U_y^{i,j,k} B_z^{i,j,k}) \tag{33}$$

$$J_y^{i,j,k} = \sigma\{\left(E_y^{i,j,k} + U_x^{i,j,k} B_z^{i,j,k}\right) - \beta\left(E_{\mathrm{x}}^{i,j,k} + \mathrm{U}_{\mathrm{y}}^{i,j,k} \mathrm{B}_{\mathrm{z}}^{i,j,k}\right)\} \tag{34}$$

$$J_z^{i,j,k} = \sigma E_z^{i,j,k} \tag{35}$$

$$\frac{1}{\rho}\frac{\partial({p_x}^{i,j,k}+{p_{h,x}}^{i,j,k})}{\partial x}+U_x\frac{\partial U_x}{\partial x}=\frac{1}{\rho}(J_y^{i,j,k}{B_z}^{i,j,k}) \tag{36}$$

$$\frac{1}{\rho}\frac{\partial({p_y}^{i,j,k}+{p_{yh,}}^{i,j,k})}{\partial y}+U_y\frac{\partial U_y}{\partial y}=\frac{1}{\rho}(J_x^{i,j,k}{B_z}^{i,j,k}) \tag{37}$$

$$\frac{1}{\rho}\frac{\partial({p_z}^{i,j,k}+{p_{h,z}}^{i,j,k})}{\partial z}+U_z\frac{\partial U_z}{\partial z}=0 \tag{38}$$

The nodes (i,j,k) are calculated based on the Maxwell and Navier–Stokes equations, and the velocity is obtained by using Eqs. (26)-(38). The x- and y-components of the magnetic flux density are negligible due to the constant magnetic flux in the device. The variation term in the Navier–Stokes equation is negligible since the system is in a steady state, and the viscous term is also negligible due to plat velocity in high Hartmann number (=113) condition.[13] These terms were ignored to increase the code calculating speed. The calculated values were used to analyze the MHD parameters to drive the circulation system. The mesh shape of the generator is shown in Fig. 4.

3. RESULTS AND DISCUSSION

To determine the power changes in the Faraday-type MHD generators, the variables were analyzed for electromagnetic, hydraulic, and geometrical parameters. The magnetic flux density is considered the primary variable because Ohm's law (Eq. (10)), the dominant equation in the device analysis, is directly affected by the magnetic field. The magnetic flux density generated from the superconducting magnet was calculated as a constant.

The current density induced by the magnetic flux density was proportional to the square of the magnetic flux density, as shown in Fig. 5. The velocity condition was 1000 m/s, and the volume of the generator was 0.00016 m^3. The 5 T of magnetic flux density satisfies the 10 kW power requirement for an electrical conductivity of 10 S/m. The electrical conductivity of 10 S/m is desirable for the plasma fluid to increase power as it is proportional to the current density as shown in Eq (16)-(18).[14] A higher magnetic flux density gives a higher power output and is therefore needed to increase efficiency. However, there are limitations in the production of an appropriate magnetic flux density. A permanent magnet cannot provide a sufficiently high magnetic flux, and an electromagnet cannot easily achieve the necessary high magnetic field conditions owing to the electrode size. Thus, a superconducting magnet was considered here to produce a sufficiently high magnetic flux density. However, a higher magnetic field increases the electromotive force and needs more superconductors. Therefore, a magnetic flux density of 5 T is applied to the MHD generator using the superconducting magnet.[7,14] The calculated power from the MHD generator, which is proportional to the square of the velocity in Eq. (23), is shown in Fig. 6. The power as a function of magnetic flux density and velocity is presented in Fig. 7. Increasing magnetic flux density and velocity causes an increase in power. The power is proportional to the cross-sectional area of the duct perpendicular to the electrode and the distance along the duct in the *x*-direction. The velocity of 1000 m/s was adopted to obtain maximum power output.[14]

The power generation, according to the duct area and duct distance, is shown in Fig. 8 and Fig. 9, respectively. For the condition of maximum constant magnetic flux density and velocity, the power has a linear relationship with the duct area and duct distance; in other words, power is linearly related to volume, implying that the power density is constant for the MHD generator. The duct area and duct distance were determined as 0.004 m^2 and 0.04 m, giving a total volume of 0.00016 m^3 to meet the power specification of 10 kW. The minimization of the volume is necessary to overcome the limits of laboratory space.

The velocity profiles for an applied magnetic flux density of 5 T and electrical conductivity of 10 S/m are shown in Fig. 10. The characteristic value of flue gas used in our simulation has a mole fraction of 72.6% nitrogen, 12.3% oxygen, 3.7% carbon dioxide, 10.5 % water, and 0.9% argon, as represented in Table 1.[15] The fluid inlet boundary condition was a velocity condition of 1000 m/s, and the outlet boundary condition was a gauge pressure condition of 0 bar. The maximum velocity of the fluid was 1170 m/s when a strong magnetic flux density was applied. The velocity was almost the same between $y = 0.0194$ m and 0.0339 m due to the magnetic flux, indicating that the viscosity of the fluid in the middle section could be negligible. The Hall effect is a negligible value because electricity is extracted in the *y*-direction, whereas Hall current is generated in the *x*-direction, which is the same direction as the fluid flow. The current density distribution based on the velocity is described in Fig. 11. The middle part of distance has a maximum current density of 53,800 A/m^2 due to the velocity distribution of the fluid channel being maximized at the middle part. In summary, the electromagnetic and geometrical parameters for achieving a 10-kW laboratory scale Faraday-type MHD generator are a magnetic flux density of 5 T, a velocity of 1000 m/s, and duct area of 0.004 m^2, where the duct distance is fixed at 0.04 m, as shown in Table 1. The power density was 62,500 kW/m^3.

The result of power density was verified compared with Sivaram's study[4] and NASA research.[16] The power density of Sivaram's thesis was 12,500 kW/m^3 with an electrical conductivity of 17 S/m, the magnetic flux density of 3.3 T, and a velocity condition of 430.3 m/s, at a temperature of 1800 K, for the argon gas. If those conditions are taken into our calculation, the power density would be 8,570 kW/m^3. The difference of 31% was due to temperature differences and type of working fluid. The condition in the NASA report was 50,000 kW/m^3 for the magnetic flux density condition of 5 T, and a velocity of 1000 m/s. The difference of 20% was caused due to the difference in electrical conductivity.

The present study is focused on the characteristic of geometrical and hydromagnetic variables, including duct geometry, velocity, and magnetic field, and does not include the heat generation. Therefore, the simulation in terms of thermal analysis is needed in future work.

4. CONCLUSIONS

Electromagnetic and geometrical variables were numerically analyzed to produce a 10-kW Faraday-type generator. The power was proportional to the square of the magnetic flux density and velocity and thus proportional to the volume of the MHD generator. The velocity and current density profile in which magnetic flux density exists in the generator are analyzed. Maximum magnetic flux density and electrical conductivity values were adopted to minimize the volume of the generator in the 10-kW condition. The total volume of the MHD device was calculated as 0.00016 m^3 to satisfy the 10 kW condition. MHD experimental generator, including electromagnets, and combustion devices will be designed using the characteristics of the variables identified in this study.

Figure captions

Figure 1 Schematic of bi-plant method using open-cycle MHD generator.

Figure 2 Schematic of a Faraday-type MHD generator.

Figure 3 Electrical circuit of the MHD generator.

Figure 4 Mesh shape of the MHD generator.

Figure 5 Power according to magnetic flux density.

Figure 6 Power according to velocity.

Figure 7 Power according to magnetic flux density and velocity.

Figure 8 Power according to duct area.

Figure 9 Power according to duct distance.

Figure 10 Velocity distribution of MHD generator.

Figure 11 The current density distribution.

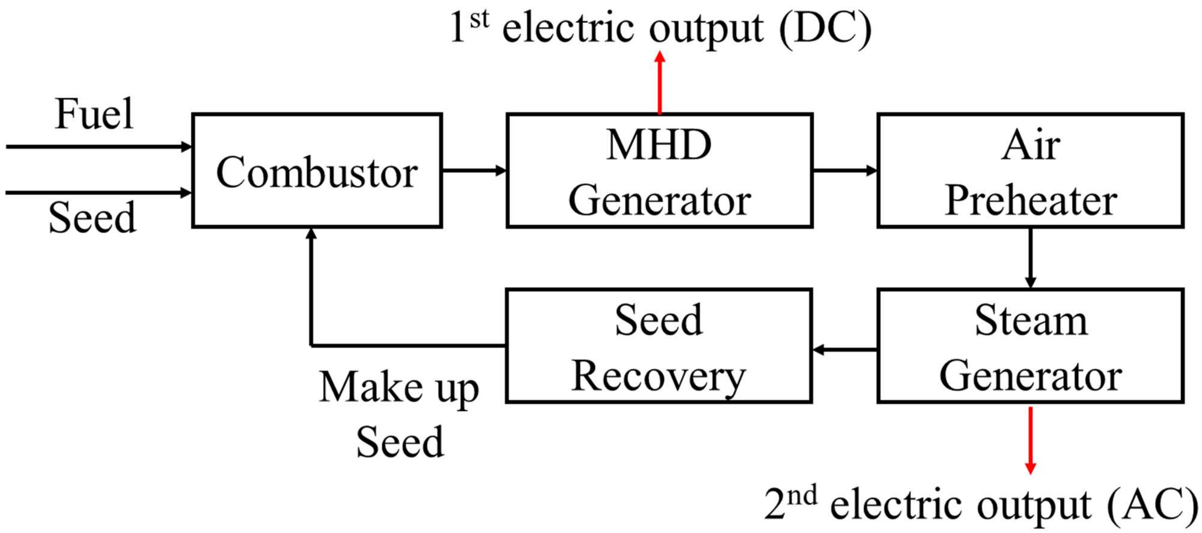

Figure 1 Schematic of bi-plant method using open-cycle MHD generator.

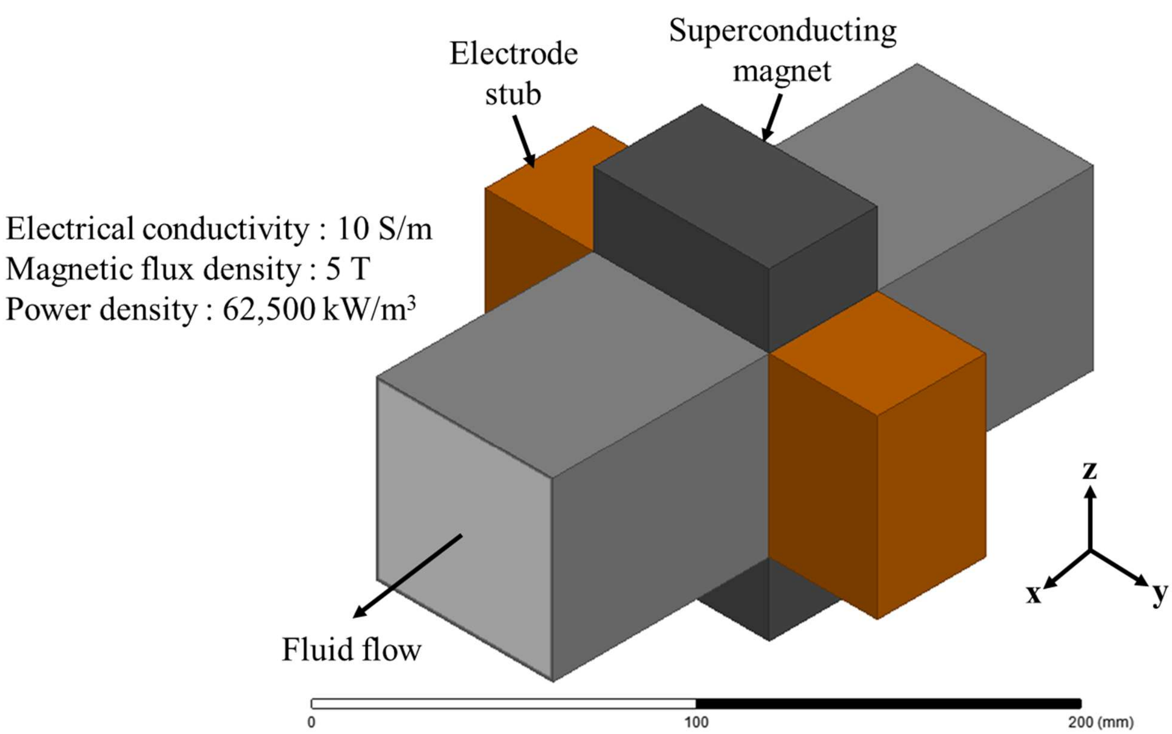

Figure 2 Schematic of a Faraday-type MHD generator.

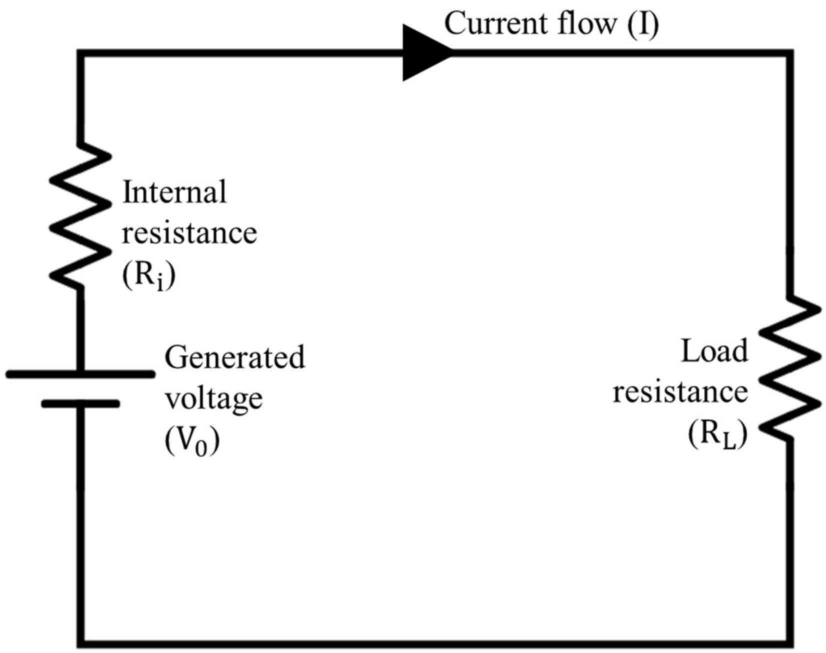

Figure 3 Electrical circuit of the MHD generator.

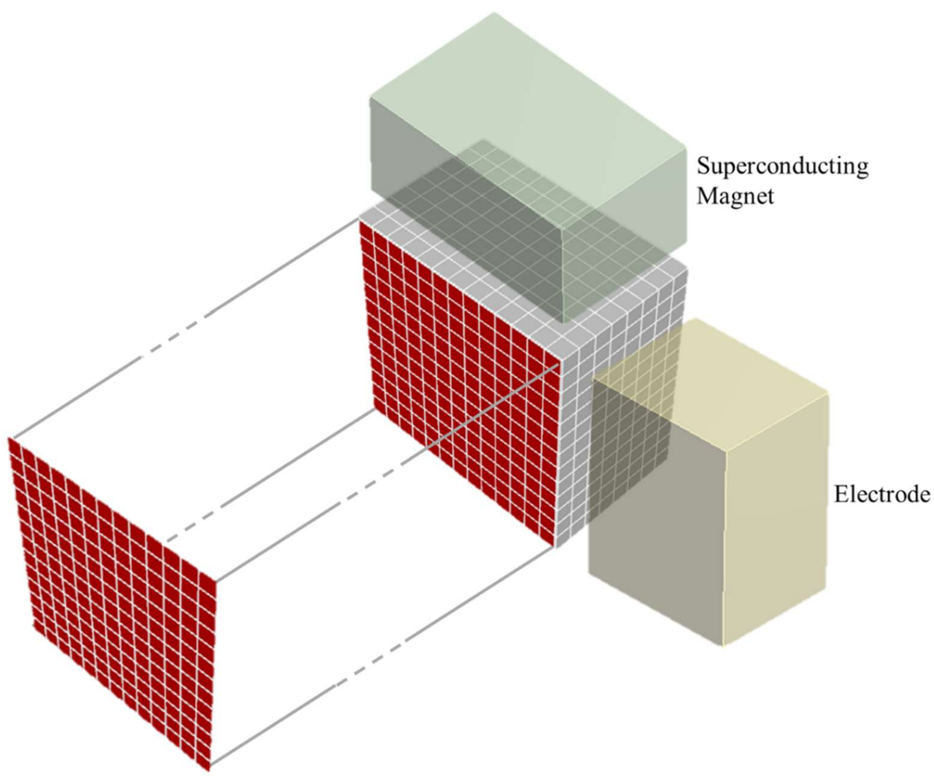

Figure 4 Mesh shape of the MHD generator.

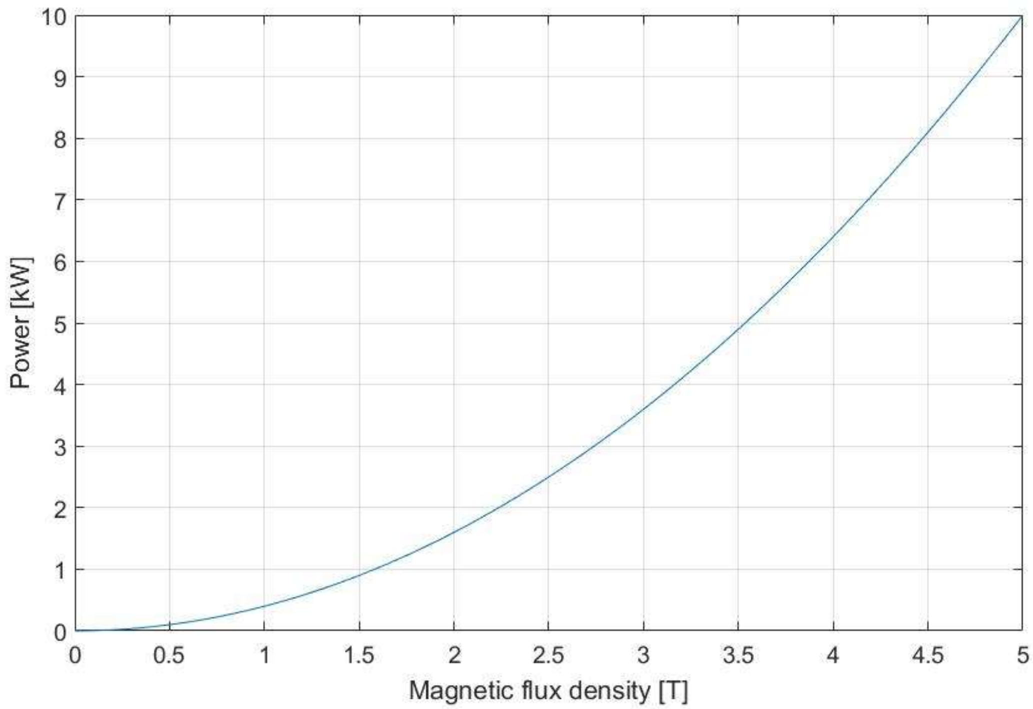

Figure 5 Power according to magnetic flux density.

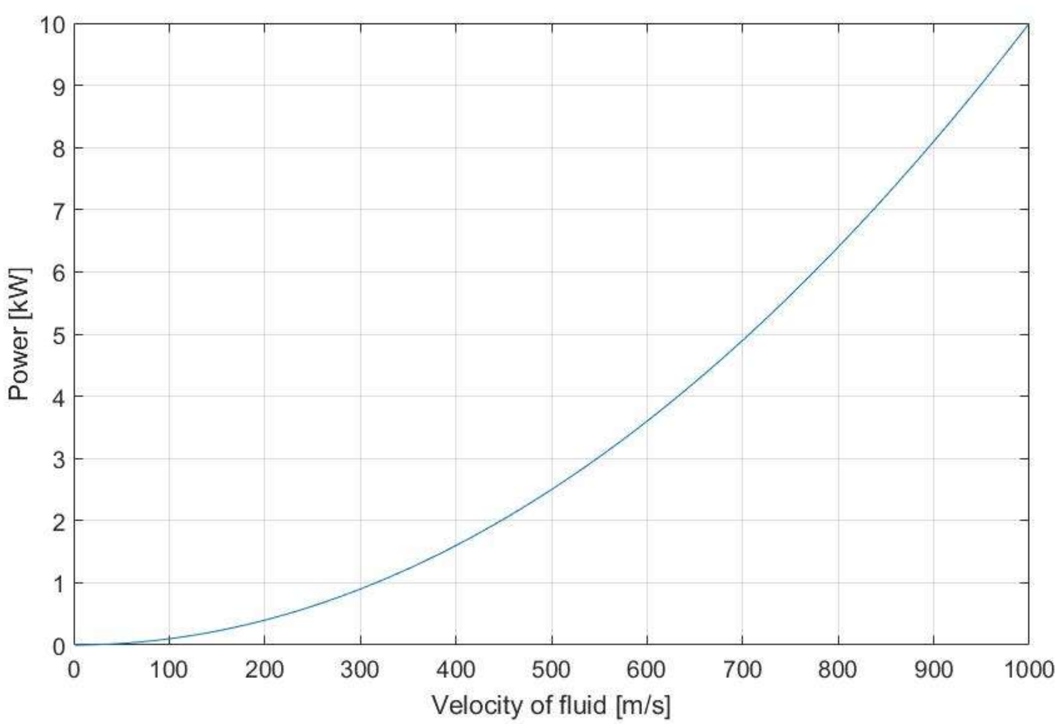

Figure 6 Power according to velocity.

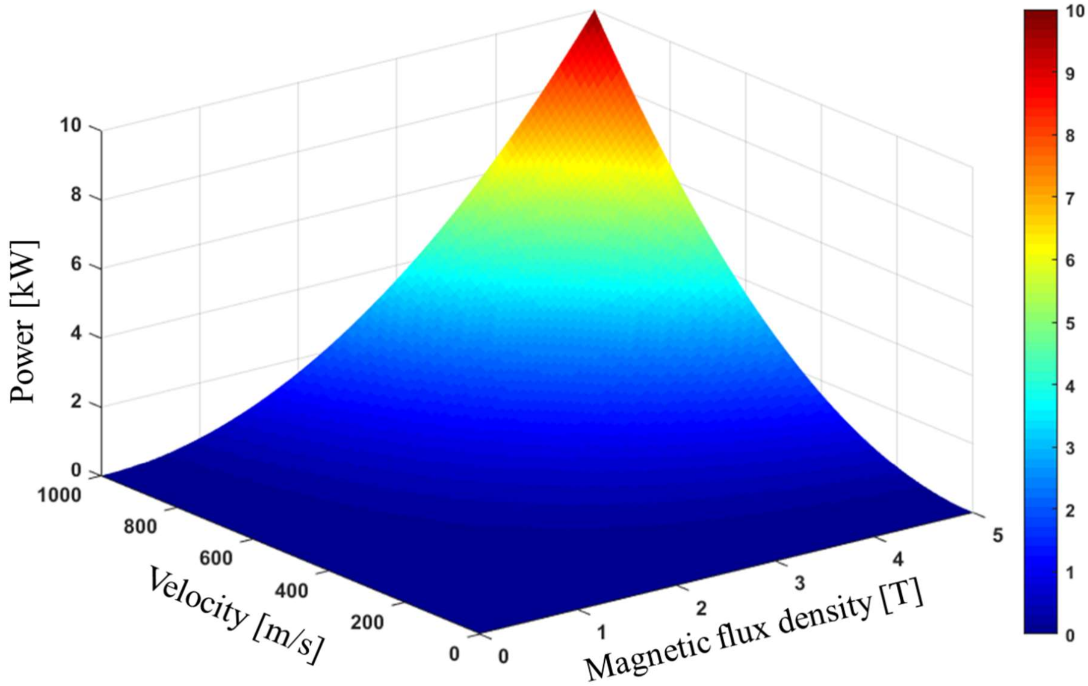

Figure 7 Power according to magnetic flux density and velocity.

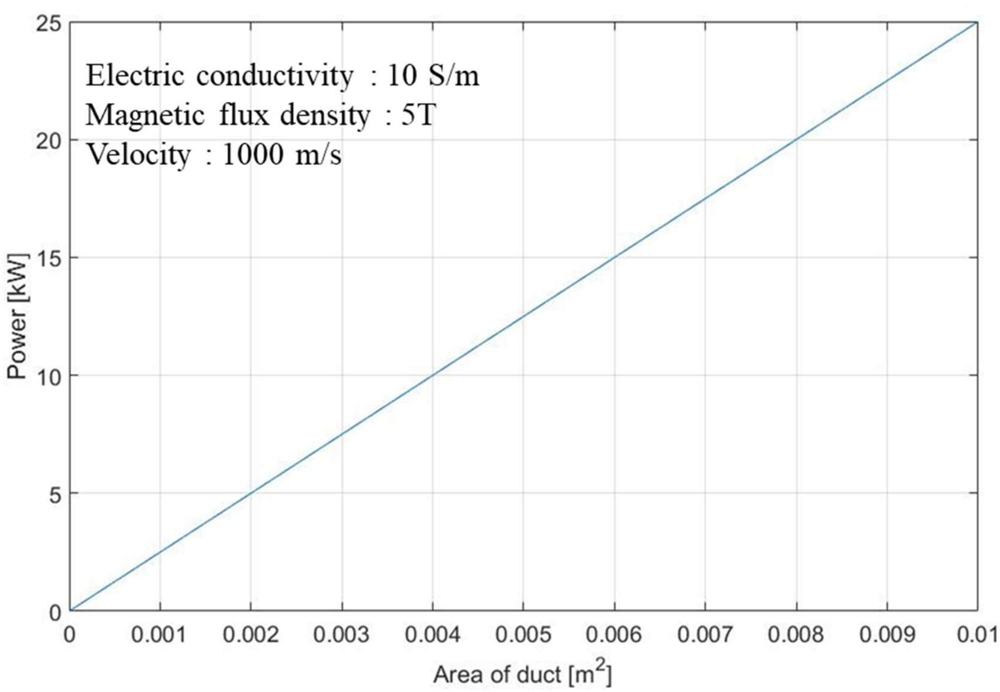

Figure 8 Power according to duct area.

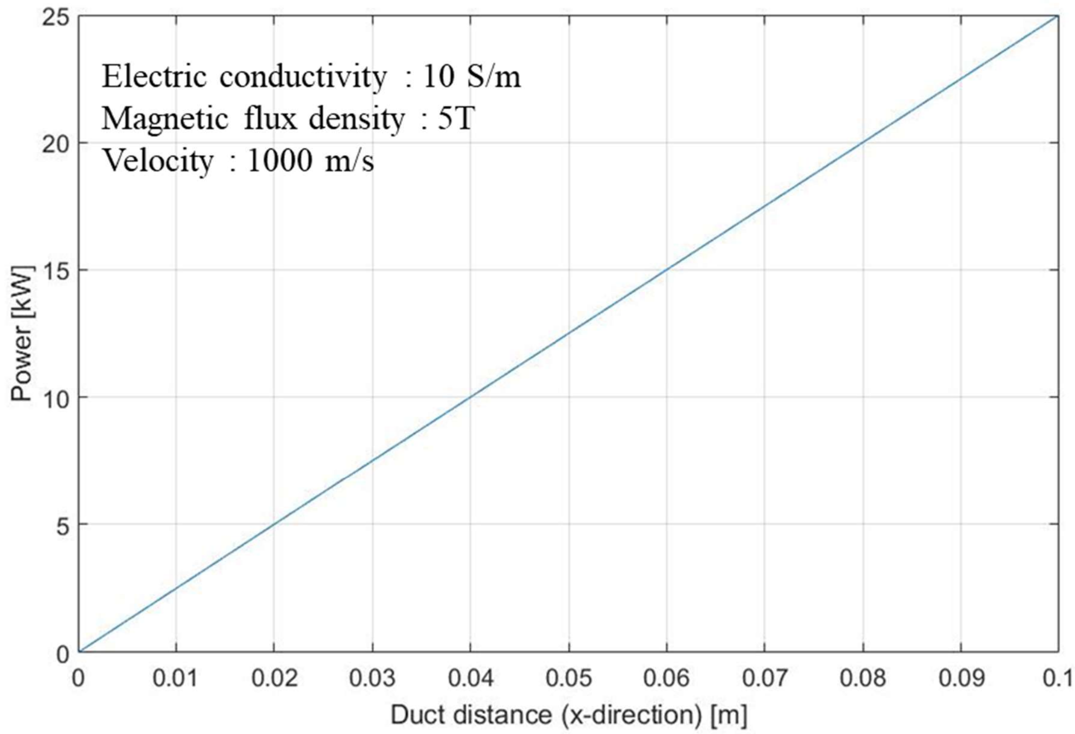

Figure 9 Power according to duct distance.

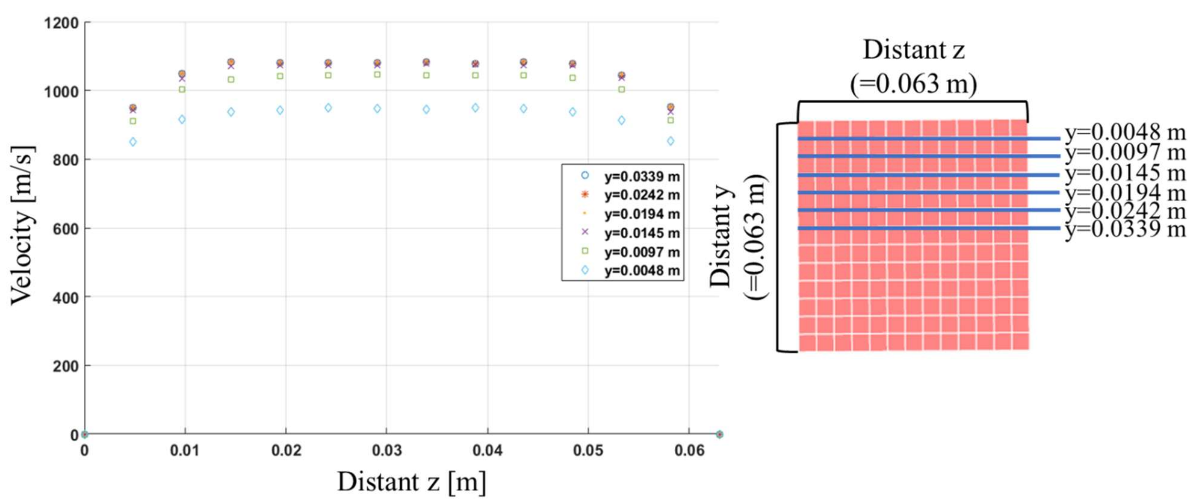

Figure 10 Velocity distribution of MHD generator.

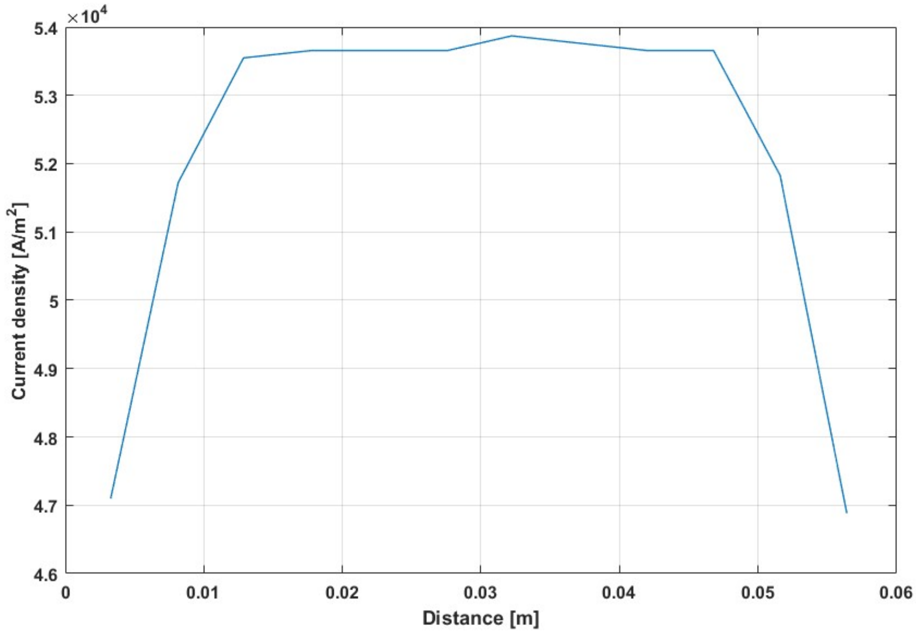

Figure 11 The current density distribution.

References

[1] Dhareppagol, Vishal D, Anand Saurav. The Future Power Generation with MHD Generators Magneto Hydro Dynamic generation…., *Int J Adv Electr Electron. Eng*. 2013; 2(6) :101-105.

[2] Alptekin E, Canakci M. Determination of the density and the viscosities of biodiesel–diesel fuel blends. *Renew. Energy.* 2008;33(12):2623-2630.

[3] Sutton GW. The Theory of Magnetohydrodynamic Power Generators (No. R62SD900). GENERAL ELECTRIC CO PHILADELPHIA PA MISSILE AND SPACE DIV 1962.

[4] Sivaram AR, Kanimozhivendhan G, Rajavel R, Durai Raj VP, Performance investigation of a closed cycle magneto hydrodynamics powerplant with liquid metal as heat source. *Indian J Sci Technol.* 2015;8(21):1-6.

[5] Celisńki ZN. Electrical equivalent circuits of DC MHD generators. *Adv Energy Convers.* 1967;7(1):67-75.

[6] Fujino T, Murakami T, Okuno Y, Yamasaki H. Experimental studies on performance of a nonequilibrium disk MHD generator with radio-frequency preionization. *IEEE Transactions Plasma Sci*. 2003;31(1):166-173.

[7] Malghan VR. History of MHD power plant development. *Energy Convers Manag*. 1996;37(5):569-590.

[8] Takahashi T, Fujino T, Ishikawa M. Comparison of generator performance of small-scale MHD generators with different electrode dispositions and load connection systems. *J Int Counc Electr Eng.* 2014;4(3):192198.

[9] Ibáñez G, Cuevas S, de Haro ML. Optimization analysis of an alternate magnetohydrodynamic generator. *Energy Convers Manage*. 2002;43(14):1757-1771.

[10] Anghaie S, Saraph G. Conceptual design analysis of an MHD power conversion system for droplet-vapor core reactors. Final report (No. DOE/ER/75871--T1). Univ. of Florida 1995.

[11] Pian CCP, McClaine AW. Techniques for the solution of MHD generator flows. *Comput Fluids.* 1984;12(4):319-338.

[12] Aithal SM, Analysis of optimum power extraction in a MHD generator with spatially varying electrical conductivity. *Int J Therm Sci.* 2008;47(8):1107-1112.

[13] Kharicha A, Molokov S Aleksandrova S, Bühler L. Buoyant convection in the HCLL blanket in a strong, uniform magnetic field. Forschungszentrum Karlsruhe 2004.

[14] Sawhney BK, Verma SS. Plant performance of a coal‐fired MHD generator. *Int J Energy Res*. 1990;14(4):433-447.

[15] Alptekin E, Canakci M. Determination of the density and the viscosities of biodiesel–diesel fuel blends. *Renew Energy.* 2008;33(12):2623-2630.

[16] Sovie, Ronald J. Closed cycle MHD power generation experiments using a helium-cesium working fluid in the NASA Lewis Facility ;1976.

Table 1 Specification of Faraday-type MHD generator

Variables	Units	Values
Temperature	K	3000
Power	kW	10
Power density	kW/m^3	62,500
Magnetic flux density	T	5
Kinematic viscosity	m^2/s	6.88×10^{-4}
Density of fluid	kg/m^3	0.114
Electrical conductivity	S/m	10
Velocity	m/s	1000
Duct area	m^2	0.004
Duct distance	m	0.04